

PHYSICAL REVIEW B

CONDENSED MATTER

THIRD SERIES, VOLUME 50, NUMBER 4

15 JULY 1994-II

Low-temperature electronic and magnetic properties of single-crystal Ni_3S_2

P. A. Metcalf

Department of Chemistry, Purdue University, West Lafayette, Indiana 47907

B. C. Crooker and M. McElfresh

Department of Physics, Purdue University, West Lafayette, Indiana 47907

Z. Kąkol

Academia Gorniczo-Hutnicza, PL-30-059, Kraków, Poland

J. M. Honig

Department of Chemistry, Purdue University, West Lafayette, Indiana 47907

(Received 10 December 1993)

Electrical transport is measured for a crystal and polycrystalline samples of Ni_3S_2 . The samples display metallic behavior with the relative resistance decreasing by more than two orders of magnitude upon cooling from 300 to 4.5 K. Low-temperature heat-capacity data are obtained by the quasiadiabatic heat-pulse method. The electronic-heat-capacity constant is determined to be $2.7 \text{ mJ/K}^2 \text{ mol}_{\text{Ni}}$. The magnetic measurements on single-crystal and polycrystalline samples yield a mass magnetic susceptibility of $0.3 \times 10^{-6} \text{ emu/g}$ [$0.4 \times 10^{-8} \text{ m}^3/\text{g}$], which is essentially temperature independent. The Pauli paramagnetic susceptibility is determined to be $5.0 \times 10^{-5} \text{ emu/mol}_{\text{Ni}}$ [$6.3 \times 10^{-10} \text{ m}^3/\text{mol}_{\text{Ni}}$], corrected for the underlying diamagnetism. Results of the electrical transport, magnetic, and heat-capacity measurements are used to characterize the electronic structure. Application of the standard theory of electron-correlation phenomena shows that Ni_3S_2 may be categorized as a good metallic conductor for which magnetic instabilities and electronic interactions are of marginal importance.

I. INTRODUCTION

Nickel sulfide, Ni_3S_2 , occurs naturally as the mineral heazlewoodite. Westgren¹ originally proposed the structure which has been more recently refined by Fleet² and Parise.³ The structure is rhombohedral, belonging to the space group $R\bar{3}2$, with lattice constants $a_r = 4.071 \text{ \AA}$, $\alpha_r = 89.459^\circ$, and $Z = 1$. It is comprised of a series of interconnected Ni_3S_2 bipyramids composed of Ni_3 triangles with apical S atoms, as shown in Fig. 1.⁴ The bipyramids are interconnected by short Ni-S and Ni-Ni distances, the distances between atoms within the bipyramids being greater than those connecting the bipyramids.^{2,3,5} This structure occurs as the low-temperature form of Ni_3S_2 and is known to be stable up to 843 K. Above 843 K, Ni_3S_2 undergoes a transition to the high-temperature, nonstoichiometric phase, $\text{Ni}_{3\pm x}\text{S}_2$, which melts incongruently above 1073 K.

We recently reported the growth of single-crystal Ni_3S_2 .⁵ No synthesis of single crystals sufficiently large for measurements of physical properties had been previously reported, other than very small crystals used for x-

ray structure investigations. Additionally, we reported the synthesis and characterization of dense polycrystalline samples.⁵ Prior research on the magnetic and transport properties of Ni_3S_2 is sparse, and measurements were based on the use of the mineral or polycrystalline

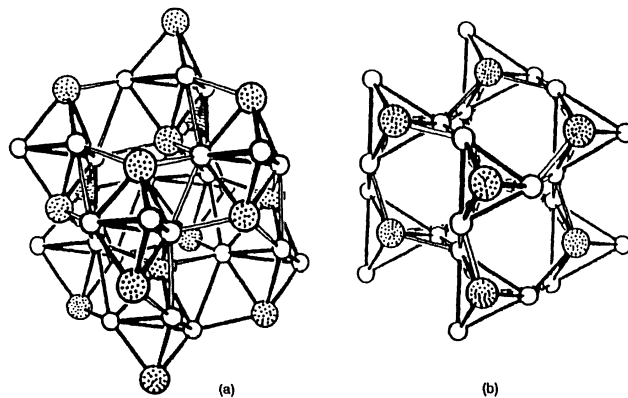


FIG. 1. Ni_3S_2 structure (a) showing interconnected bipyramids, (b) viewed down the crystallographic threefold axis (Ref. 7).

material. The mineral heazlewoodite has a reported iron impurity content of 0.56 wt %, and its occurrence in nature is rare. The room-temperature resistivity for the naturally occurring mineral was stated to be $1.5 \times 10^{-5} \Omega \text{ cm}$.⁶ Yagi and Wagner⁷ reported the results of electrical conductivity measurements on a polycrystalline sample for the temperature range between 100 and 750°C. The resistivity for the low-temperature phase was shown to vary linearly with temperature up to the transition temperature, at which point there is a sudden increase in the resistivity. The magnetic properties of a polycrystalline sample of Ni_3S_2 were measured in the temperature range of 80–300 K.⁸ The magnetic susceptibility was found to be temperature independent, with a reported value of $0.6 \times 10^{-6} \text{ emu/g}$ [$0.8 \times 10^{-8} \text{ m}^3/\text{kg}$]. Thus, the material was classified as Pauli paramagnetic.

Heat-capacity results for Ni_3S_2 were first published by Weller and Kelley⁹ for the temperature range 55–300 K. Results in the high-temperature range of 298–1250 K were reported by Ferrante and Gokcen.¹⁰ More recently, results for the temperature range of 8.7–976 K were published by Stølen *et al.*¹¹ There is a regular increase of the heat capacity from 10–834 K, above which the high-temperature phase occurs. Stølen *et al.* reported that a fit of the low-temperature heat capacity to a C_p/T versus T^2 relation yielded an electronic-heat-capacity constant equal to zero within experimental accuracy.

We report the results for the measurement of the low-temperature electrical transport, magnetic properties for single-crystal and polycrystalline Ni_3S , and measurements of the heat capacity for polycrystalline Ni_3S_2 . Results of these investigations are used to characterize the electronic structure.

II. EXPERIMENTAL

A. Preparation and characterization of samples

The synthesis and structural characterization of Ni_3S_2 single crystals and polycrystalline material has been reported in detail elsewhere.⁵ A “melt-quench” technique was used to produce polycrystalline boules of Ni_3S_2 which were brass yellow in appearance. Single crystals of Ni_3S_2 were grown by a vapor transport technique. The crystals were brass yellow in appearance and exhibited metallic luster. The nickel to sulfur ratio for several single crystals was characterized using an electron probe microanalyzer. The crystals were very homogeneous; there was no indication of inclusions of nickel, sulfur, or other nickel-sulfide phases within the limit of detection. The composition was found to be $59.79 \pm 0.26 \text{ at. \% Ni}$ to $40.21 \pm 0.26 \text{ at. \% S}$, corresponding to stoichiometric $\text{Ni}_{3.0}\text{S}_{2.0}$. There were no impurities found within the detection limit using energy dispersive analysis by x rays. The x-ray powder diffraction values obtained from patterns for the single-crystal and polycrystalline material measurements corresponded well to the calculated and reported values.^{2,5} The crystals were examined by transmission electron microscopy; no short-range defects or disorder were observed. Single-crystal x-ray refinement confirmed the structure to be that reported for heazlewoodite.^{2,3,5}

B. Electrical conductivity measurements

The conductivity was measured for a Ni_3S_2 crystal using the four-probe van der Pauw technique.¹² The contacts were formed by evaporating silver metal pads onto which copper wires were attached with silver paint. The conductivity was measured as a function of temperature between 300 and 4.5 K. The conductivity of the polycrystalline material was measured using the standard four-probe method. Rectangular bars were cut from the melt-quenched boules with dimensions of approximately $2 \times 1 \times 0.5 \text{ mm}^3$. Copper wires were attached to silver paint contacts.

C. Magnetic susceptibility measurements

The magnetic properties of the polycrystalline and single-crystal Ni_3S_2 were measured using a vibrating sample magnetometer (VSM) and a superconducting quantum interference device (SQUID) magnetometer, respectively. The small magnitude of the signal and small size of the crystals mandated the use of the SQUID magnetometer for the single-crystal magnetic measurements, since it is by far the more sensitive of the two techniques.

The VSM used in this study was a Princeton Applied Research 155 magnetometer. Rectangular bars of approximately $1 \times 1 \times 3 \text{ mm}^3$ were cut from the polycrystalline boules for VSM measurements. The polycrystalline sample was cooled in zero field down to 4.5 K and the magnetization was measured as a function of increasing field strength up to 6 kOe [0.5 A/m]. The field was again set to zero and the sample was warmed to a higher temperature. In this manner, measurements were taken as a function of field for a number of temperatures between 4.5 K and room temperature.

Magnetization measurements for the crystals were made using a Quantum Design SQUID magnetometer. Measurements were taken by increasing the temperature from 4.5 to 350 K at a given field, then changing the field to a higher value and taking measurements as the temperature was decreased down to 4.5 K. By this method, measurements were obtained for the magnetization of the crystals from 4.5–350 K in magnetic fields up to 55 kOe.

D. Heat capacity measurements

Specific-heat measurements for the polycrystalline samples were taken in a ^3He cryostat using the quasiadiabatic heat-pulse method. Data were collected in the temperature range from 25–0.5 K, on a rectangular bar with dimensions of about $0.6 \times 1.0 \times 0.4 \text{ cm}^3$, which was cut from a melt-quenched boule.

III. RESULTS AND DISCUSSION

A. Conductivity

The results of the electrical transport measurements on polycrystalline and single-crystal Ni_3S_2 were very similar. Measurements of resistivity as a function of temperature are presented in Fig. 2(a) for a single crystal and Fig. 2(b) for a polycrystalline sample. These results were found to

be reversible. Consistent with the crystal structure, no anisotropy was noted in the single-crystal measurement. The room-temperature resistivity for the single crystal was about $1.8 \times 10^{-5} \Omega \text{ cm}$; this is comparable to that reported for the naturally occurring mineral ($1.5 \times 10^{-5} \Omega \text{ cm}$).⁶ The room-temperature resistivity for the melt-quenched sample was about $1.1 \times 10^{-4} \Omega \text{ cm}$, comparable to that previously reported for polycrystalline samples ($1.5 \times 10^{-4} \Omega \text{ cm}$ at 100°C).⁷ The resistivity decreased by more than two orders of magnitude upon cooling the sample from room temperature to 4.5 K. The variation of resistivity with temperature is almost linear at higher temperatures, as shown in Fig. 3(a). At temperatures below 50 K, the resistivity shows a T^3 dependence, see Fig. 3(b). The residual resistivity for the single-crystal Ni_3S_2 was approximately $1.0 \times 10^{-7} \Omega \text{ cm}$.

Based on these results, Ni_3S_2 would be classified as a Class IIIB mixed valence compound, in accordance with the classification scheme proposed by Day and Robin.¹³ Class IIIB mixed valence compounds contain like atoms in identical environments with fractional formal oxidation states and delocalized electrons. These compounds display metallic conductivity as the result of electron delocalization throughout the solid. In Ni_3S_2 , the nickel atoms are in identical environments, as determined by structural studies.^{2,3,5} The oxidation states of the nickel ions can be thought of as two Ni^{1+} and one Ni^{2+} per formula unit, but a formal oxidation state of $+4/3$ for each

nickel is more representative of the electron delocalization. The metallic conductivity confirms that the electrons are delocalized throughout the solid, showing that the electrons are free to move between Ni_3 clusters.

B. Magnetic susceptibility

The results of magnetic measurements performed on polycrystalline and single crystals of Ni_3S_2 were virtually the same for both types of samples. A small amount (>0.00001 at. %) of ferromagnetic nickel produced minor interference in the magnetic measurements for a few of the samples. In these instances, the M vs H characteristics of the samples were used to determine the magnetization from the ferromagnetic nickel, and minor corrections were applied. The mass magnetic susceptibility for Ni_3S_2 is essentially temperature independent, with a value of $\chi_g = 0.3 \times 10^{-6} \text{ emu/g}$ [$0.4 \times 10^{-8} \text{ m}^3/\text{kg}$], as shown in Fig. 4; this is one half of the previously reported value of $\chi_g = 0.6 \times 10^{-6} \text{ emu/g}$ [$0.8 \times 10^{-8} \text{ m}^3/\text{kg}$].⁸ The low value of the mass magnetic susceptibility and its negligible variation with temperature are consistent with an interpretation of the magnetic properties of Ni_3S_2 as arising from Pauli paramagnetism. The molar magnetic susceptibility was calculated to be $7.2 \times 10^{-5} \text{ emu/mol}_{\text{Ni}_3\text{S}_2}$ [$9.0 \times 10^{-10} \text{ m}^3/\text{mol}_{\text{Ni}_3\text{S}_2}$]. The measured

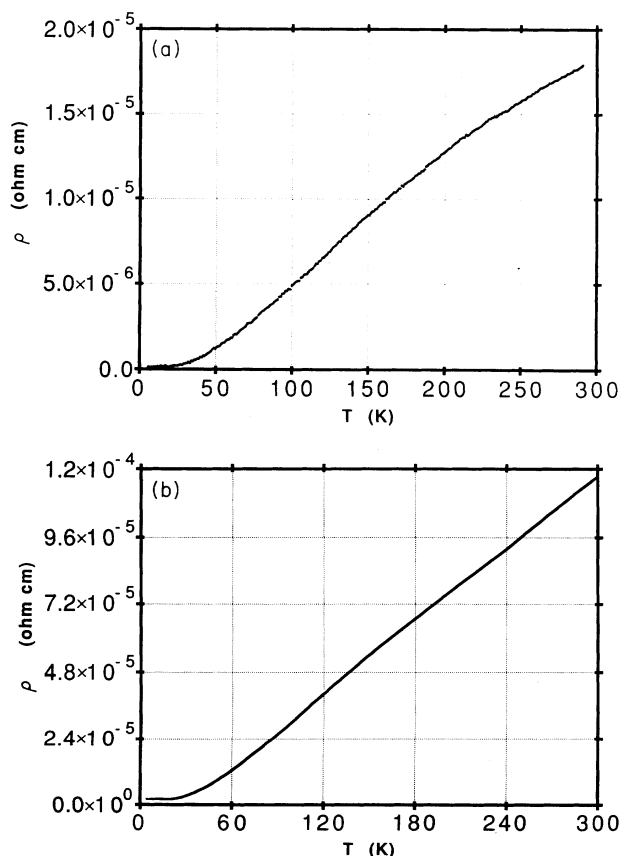


FIG. 2. (a) Resistivity versus temperature data for single-crystal Ni_3S_2 . (b) Resistivity versus temperature data for polycrystalline Ni_3S_2 .

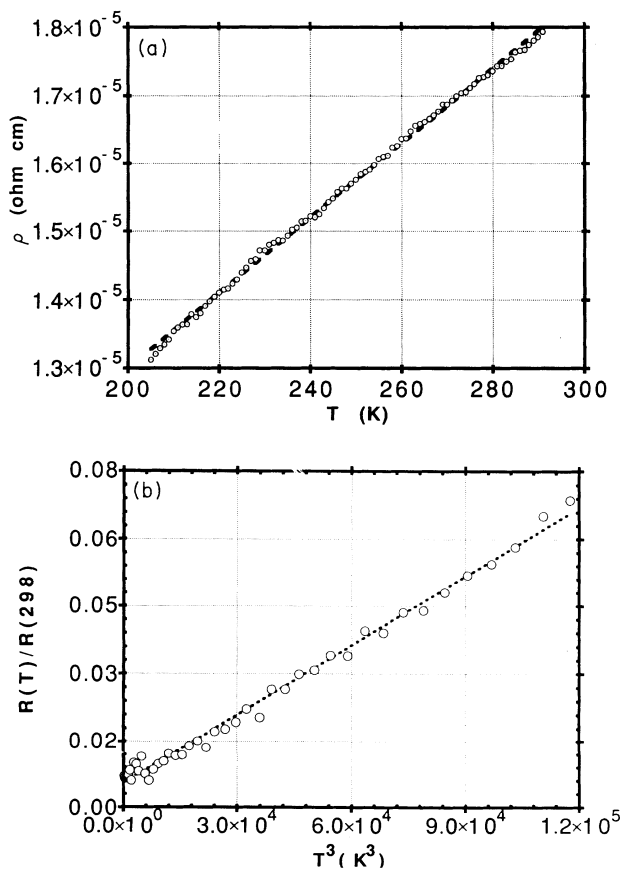


FIG. 3. (a) High-temperature T^1 relation of resistivity for single-crystal Ni_3S_2 . (b) Low-temperature T^3 relation of resistivity for single-crystal Ni_3S_2 .

molar magnetic susceptibility is actually a combination of the Pauli paramagnetic susceptibility with the Landau and Larmor diamagnetic susceptibilities. Methods for approximating the Landau and Larmor contributions have been proposed by several authors.¹⁴ Application of these methods led to the approximate values of $\chi_{\text{Landau}} = -5.0 \times 10^{-5}$ emu/mol_{Ni₃S₂} [-6.3×10^{-10} m³/mol_{Ni₃S₂}], $\chi_{\text{Larmor}} = -2.8 \times 10^{-5}$ emu/mol_{Ni₃S₂} [-3.5×10^{-10} m³/mol_{Ni₃S₂}], and $\chi_{\text{Pauli}} = 1.5 \times 10^{-4}$ emu/mol_{Ni₃S₂} [1.9×10^{-10} m³/mol_{Ni₃S₂}] or 5.0×10^{-5} emu/mol_{Ni} [6.3×10^{-10} m³/mol_{Ni}].

The Pauli paramagnetic susceptibility derives from a small alteration in orbital occupancy resulting from the splitting of the spin-up and spin-down energy levels in a magnetic field. The effect is proportional to the density of states at the Fermi level. The volume magnetic susceptibility for Pauli paramagnetic magnetic materials is given by¹⁵

$$\chi_{\text{Pauli}} = (g^2 \mu_b^2 / 2) \rho_0(\epsilon_F),$$

where g is the Landé factor and μ_b is the Bohr magneton. Using this relation, the density of states at the Fermi level for Ni₃S₂ in the ground state was calculated as $\rho_0(\epsilon_F) = 6.8 \times 10^{22}$ eV⁻¹ cm⁻³ (assuming $g = 2.00$).

C. Heat capacity

No peaks in the heat capacity were observed for the measured temperature range. In the lowest-temperature region, $T < 6$ K, the heat capacity was fit to the linear relation

$$C_p / T = \alpha T^2 + \gamma.$$

The least-squares regression, optimized parameter fit yields $\alpha = 0.2$ mJ/mol_{Ni₃S₂} and $\gamma = 8.1$ mJ/mol_{Ni₃S₂} K², as shown in Fig. 5. A Debye temperature of $\theta_D = 398 \pm 5$ K was calculated, which compares well with those determined for typical metals.¹⁵ The linear relationship for the determination of the electronic- and lattice-heat-

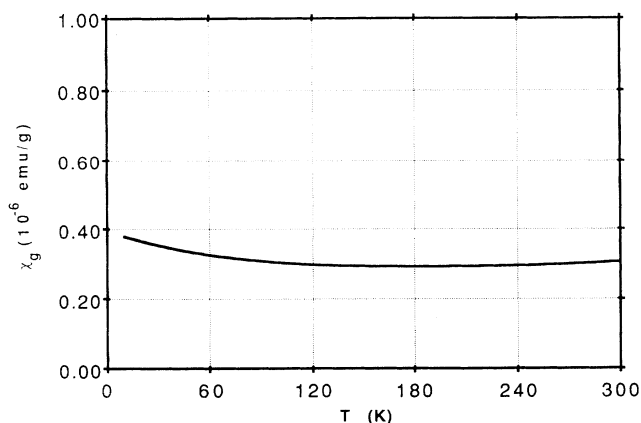


FIG. 4. Field-independent χ_g vs T data for single-crystal Ni₃S₂.

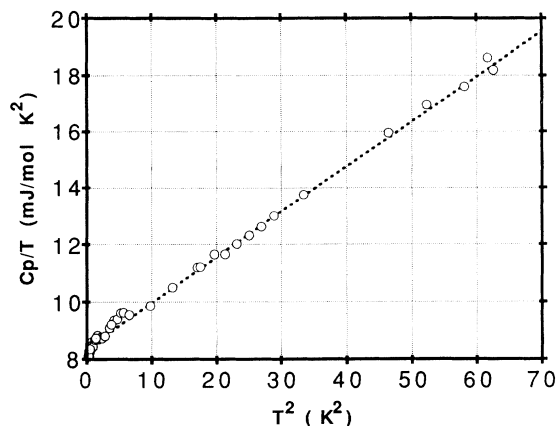


FIG. 5. Fitting of low-temperature heat-capacity data to the relation $C/T = \alpha T^2 + \gamma$.

capacity constants should be fit at temperatures lower than $\theta_D/50$; thus, the temperature range chosen for the fit was appropriate.

The value of the electronic-heat-capacity constant, $\gamma = 8.1$ mJ/mol_{Ni₃S₂} K² or 2.7 mJ/mol_{Ni} K², is consistent with those reported for standard metals.¹⁵ This is in contrast to that reported by Stølen *et al.* in which they determined the electronic-heat-capacity constant by extrapolation from 10 K to be equal to zero.¹¹ Figure 6 is a compilation of our data with those taken by Ferrante and Gokcen,¹⁰ Weller and Kelley,⁹ and Stølen *et al.*¹¹ The present measurements extrapolate well to the previously reported values (see insert).

D. Electronic structure

Ni₃S₂ can also be classified as a simple metal. The class of simple metals contains a small number of transition-metal compounds for which the unmodified free-electron theory may be used as a framework for interpreting their physical properties. This is based on band-structure effects involving conduction bands formed from atomic d

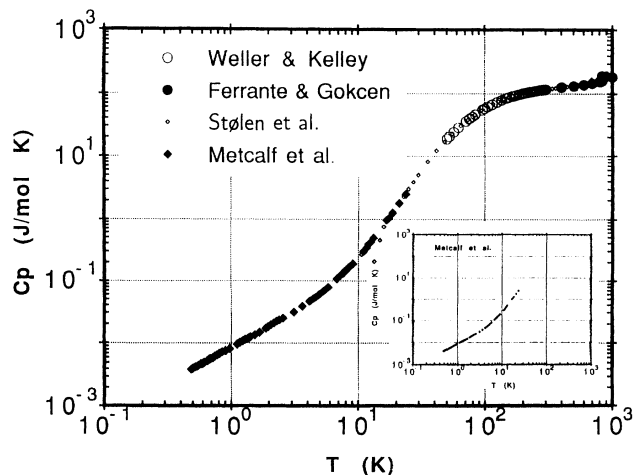


FIG. 6. Compilation of heat-capacity data for Ni₃S₂; inset shows data from this study.

orbitals. For free-electron metals, a derivation originally provided by Sommerfeld, based on the Fermi-Dirac distribution, leads to¹⁵

$$C_E/T = \gamma = (\pi^2/3)k_b^2\rho_0(\epsilon_F).$$

The density of states at the Fermi level for the ground state of Ni₃S₂ was determined from the above relation to be $5.0 \times 10^{22} \text{ eV}^{-1} \text{ cm}^{-3}$. This value compares reasonably well with the value determined for the Pauli susceptibility, $6.8 \times 10^{22} \text{ eV}^{-1} \text{ cm}^{-3}$, indicating that the corrections made for the diamagnetic contributions are of the appropriate magnitude.

The results of the electrical transport, magnetic, and heat-capacity measurements may be used to characterize the electronic structure. Models for the electronic structure of metal sulfides have often been based either on the molecular-orbital theory, which best describes localized phenomena, or on band theory, which best describes delocalized phenomena. However, most transition-metal chalcogenides and oxides exhibit intermediate properties, neither strictly localized or delocalized. Instead, there exists a competition between factors that favor delocalization (such as the bonding overlap of atomic orbitals in the solid) and factors that favor localization (such as the Coulomb repulsion between electrons or their interaction with defects or vibrational modes in the lattice).

One theory presented to deal quantitatively with this problem was the Mott-Hubbard model.¹⁶ In this model, the type of ground state encountered for a half-filled *d* band depends on the ratio U/W , where U is the Coulomb repulsion energy between two electrons of opposite spins in the same state and W is the bandwidth. For $U \gtrsim W$, the energy required to pair electrons on the metal *d* orbitals is larger than the energy gained by allowing the electrons to form bands. Thus, the band splits into two subbands, resulting in a semiconducting or insulating ground state, as seen in Figure 7. For $U \lesssim W$, the subbands overlap, yielding a metallic ground state with the Fermi level in the middle of the partially filled band. The Mott-Hubbard model has been reformulated in a theory developed by Gutzwiller, Brinkman and Rice, Spalek and co-workers, as well as others.¹⁷ In this theory, the interacting electrons are replaced by a set of independent quasiparticles. The theory has been shown to be useful for characterizing the properties of metals that display correlated electron behavior.

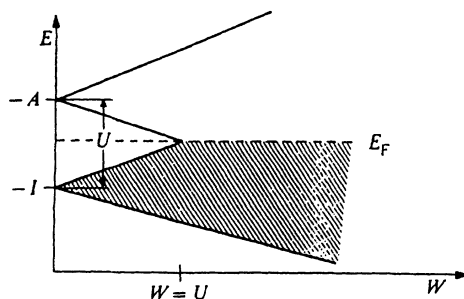


FIG. 7. Hubbard subbands, as a function of bandwidth (Ref. 5).

One result of the theory is to illustrate how the experimentally determined quantities γ and χ_P are useful for characterizing correlation effects. From the theory one finds that the electronic contribution to the heat capacity of correlated electrons is given by

$$\gamma = \gamma_0 / (1 - I^2), \quad I \equiv U/U_c,$$

where γ_0 is the free-electron value of γ , and U_c is the critical value of the intra-atomic Coulomb interaction energy U , above which there are no double occupancies. A material remains metallic as long as $I < 1$. Similarly, it may be shown that the Pauli paramagnetic susceptibility for a correlated electron system is given by

$$\chi_P = \chi_0 / (1 - I^2) S,$$

where χ_0 is the free-electron Pauli paramagnetic susceptibility, and S is the Stoner enhancement factor. The theory is based on two assumptions that somewhat limit its applicability; it assumes half-filled bands and a rectangular density of states. Taking into account the limitations of the theory, the Stoner enhancement factor may be defined as

$$S = 1 - 2I[1 + I/2]/(1 + I)^2.$$

The so-called inverse Wilson ratio (R^{-1}) can then be calculated from the following relationships:

$$R^{-1} = \gamma / \chi_P = (\gamma_0 / \chi_0) S,$$

$$\gamma_0 = 2/3 \pi^2 k_b^2 \rho_0(\epsilon_F),$$

$$\chi_0 = 1/2 g^2 \mu_b^2 \rho_0(\epsilon_F),$$

where the inverse Wilson ratio (R^{-1}) is in cgs units, k_b is the Boltzmann constant, μ_b is the Bohr magneton, and $\rho_0(\epsilon_F)$ is the free-electron density of states per spin per site at the Fermi level. The resulting value for the inverse Wilson ratio, with the Landé g factor taken to be equal to 2, is

$$R^{-1} = \gamma / \chi_P = (7.2894 \times 10^8) S,$$

where the numerical factor is based on the use of the cgs system. It is now evident that the Stoner enhancement factor (S) is accessible from the experimentally determined values for γ and χ_P .

From the above relation for the Stoner factor, one may determine I . In turn, the value of I may be used to determine the effective-mass enhancement ratio (m^*/m_b) via the relation

$$m^*/m_b = 1/(1 - I^2),$$

where m^* is the effective mass of the correlated electrons and m_b is the free-electron band mass. An important result of the theory is that the effective mass of the charge carriers increases as the bandwidth diminishes. Here, Φ is interpreted as a bandwidth reduction factor, and has been shown to be inversely proportional to the effective mass

$$\Phi = (m^*/m_b)^{-1} = 1 - I^2.$$

It can be seen from the above relations that S , Φ , and m^*/m_b approach unity as the value U/U_c diminishes, that is, as the degree of electron correlation diminishes.

Since Ni_3S_2 exhibits a bronze metallic luster and metallic conductivity, application of the results of the above-mentioned theory to the Ni_3S_2 system is expected to yield results indicative of a low degree of electron correlation, that is, $\Phi \approx 1$, $S \approx 1$, and $m^*/m_b \approx 1$.

As determined in this study, $\gamma = 2.7 \times 10^4 \text{ erg/K}^2 \text{ mol}_{\text{Ni}}$ [$8.1 \text{ mJ/mol}_{\text{Ni}} \text{ K}^2$], and $\chi_P = 5.0 \times 10^{-5} \text{ emu/mol}_{\text{Ni}}$ [$6.3 \times 10^{-10} \text{ m}^3/\text{mol}_{\text{Ni}}$]. Using the above relations, values of $R = 5.4 \times 10^8$ for the inverse Wilson ratio and $S = 0.74$ for the Stoner enhancement factor may be determined. These values show the Ni_3S_2 system to be far removed from the magnetic instability that sets in as S approaches zero. From the Stoner enhancement factor a value of $I = 0.16$ is determined. Accordingly, the band narrowing factor is found to be 0.97, quite close to the $\Phi = 1$ expected for a free-electron gas. The effective-mass enhancement ratio is found to be $m^*/m_b \approx 1.0$. This indicates that the Ni_3S_2 electronic properties are not far removed from those anticipated for a standard metal.

The density of states at the Fermi level for Ni_3S_2 , determined from the heat capacity, is $0.40 \text{ eV}^{-1} \text{ spin-site}^{-1}$; this includes a correction due to the fact that the formal valence of Ni in Ni_3S_2 is $+4/3$. This value may be used to estimate a bandwidth (W) of 2.5 eV, which is comparable to the bandwidths encountered for $3d$ metals. Finally, using the relationship for a rectangular density of states,

$$I = U/2W,$$

a value of $U = 0.80 \text{ eV}$ was determined for the intra-atomic Coulomb repulsion. This value is non-negligible, but not nearly as large as the values $U \approx 3\text{--}6 \text{ eV}$ encountered for many $3d$ transition-metal sulfides.

IV. CONCLUSION

Electrical transport measurements have shown Ni_3S_2 to be a good metallic conductor, with a room-temperature resistivity of about $1.8 \times 10^{-5} \Omega \text{ cm}$, which decreases by more than two orders of magnitude upon cooling to 4.5 K. Magnetization measurements have shown Ni_3S_2 to display Pauli paramagnetic behavior with a temperature-independent susceptibility of $0.3 \times 10^{-6} \text{ emu/g}$ [$0.4 \times 10^{-8} \text{ m}^3/\text{kg}$] and a Pauli paramagnetic susceptibility of $5.0 \times 10^{-5} \text{ emu/mol}_{\text{Ni}}$ [$6.3 \times 10^{-10} \text{ m}^3/\text{mol}_{\text{Ni}}$]. Heat-capacity measurements yielded a Debye temperature of 398 K and an electronic-heat-capacity constant of $2.7 \times 10^{-3} \text{ J/K}^2 \text{ mol}_{\text{Ni}}$.

It has been shown by a standard analysis involving the theory of electron correlation phenomena that Ni_3S_2 falls into the category of a good metallic conductor for which magnetic instabilities and electronic interactions are of only marginal importance.

ACKNOWLEDGMENTS

The authors wish to thank J. Spałek and A. W. Overhauser for helpful discussions. This research was supported in part by MISCON at Purdue University on Grant No. DE-FG02-90ER45427, and in part by ACS-PRF Grant No. 22396-AC3-C.

¹A. Westgren, *Z. Anorg. Allg. Chem.* **239**, 82 (1938).

²M. E. Fleet, *Am. Mineral.* **62**, 341 (1977).

³J. P. Parise, *Acta Crystallogr. Sec. B* **36**, 1179 (1980).

⁴J. H. El Nakat, I. G. Dance, K. J. Fisher, D. Rice, and G. D. Willett, *J. Am. Chem. Soc.* **113**, 5141 (1991).

⁵P. A. Metcalf, P. Fanwick, Z. Kakol, and J. M. Honig, *J. Solid State Chem.* **104**, 81 (1993).

⁶Gmelin, *Handb. Anorg. Chem.* **57**, Ni [B] 631 (1986).

⁷H. Yagi and J. B. Wagner, *Oxid. Met.* **18**, 41 (1982).

⁸D. M. Pasquariello, R. Kershaw, J. D. Passaretti, K. Dwight, and A. Wold, *Inorg. Chem.* **23**, 872 (1984).

⁹W. W. Weller and K. K. Kelley, *U.S. Bur. Mines Rep. Invest.* **1964**, 6511.

¹⁰M. J. Ferrante and N. A. Gokcen, *U.S. Bur. Mines Rep. Invest.* **1982**, 8745.

¹¹S. Stølen, F. Grønvdal, E. Westrum Jr., and G. Kolonin, *J. Chem. Thermodyn.* **23**, 77 (1991).

¹²L. J. van der Pauw, *Philips Res. Rep.* **13**, 1 (1958).

¹³M. B. Robin and P. Day, *Adv. Inorg. Chem. Radiochem.* **10**,

247 (1966).

¹⁴R. S. Drago, *Physical Methods in Chemistry* (Saunders, Philadelphia, 1977); P. W. Selwood, *Magnetochemistry* (Interscience, New York, 1956).

¹⁵C. Kittel, *Introduction to Solid State Physics* (Wiley, New York, 1976); P. A. Cox, *The Electronic Structure and Chemistry of Solids* (Oxford Science, Oxford, England, 1987); N. Ashcroft and D. N. Mermin, *Solid State Physics* (Saunders, Philadelphia, 1976).

¹⁶N. F. Mott, *Metal-Insulator Transitions* (Taylor & Francis, London, 1974); J. Hubbard, *Proc. R. Soc. London Ser. A* **281**, 401 (1964).

¹⁷M. C. Gutzwiller, *Phys. Rev. Lett.* **10**, 159 (1963); *Phys. Rev.* **137**, A1726 (1965); W. F. Brinkman and T. M. Rice, *Phys. Rev. B* **2**, 4302 (1970); J. Spałek, A. Datta, and J. M. Honig, *Phys. Rev. Lett.* **59**, 728 (1987); J. Spałek, M. Kokowski, and J. M. Honig, *Phys. Rev. B* **39**, 4175 (1989); J. Spałek, *J. Solid State Chem.* **88**, 70 (1990).